ChemComm

Accepted Manuscript

This article can be cited before page numbers have been issued, to do this please use: S. Biswas, R. Y, S. Barman, M. Bera, A. Paul, M. Mandal and P. N.D. Singh, *Chem. Commun.*, 2018, DOI: 10.1039/C8CC01854E.

ROYAL SOCIETY OF CHEMISTRY

rsc.li/chemcomm

View Article Online
DOI: 10.1039/C8CC01854E

ChemComm

COMMUNICATION

A Dual-Analyte Probe: Hypoxia Activated Nitric Oxide Detection with Phototriggered Drug Release Ability

Received 00th January 20xx,
Accepted 00th January 20xx

DOI: 10.1039/x0xx00000x

www.rsc.org/

Sandipan Biswas,[a] Y. Rajesh,[b] Shrabani Barman,[a] Manoranjan Bera[a], Amrita Paul[a], Mahitosh Mandal,[b] N.D. Pradeep Singh[a]*

A new strategy for the detection of hypoxia and NO succeeded by photocontrolled delivery of anticancer agent has been demonstrated. The developed system is able to produce distinct responses (dual channel) upon interaction with hypoxia and NO. This probe can also release anticancer drug upon photoirradiation acting potentially as both dual-analyte imaging agent and prodrug.

Hypoxia is evolving as a primary target in the development of activatable chemotherapeutic prodrugs.[1, 2] Hypoxia is one of the unique features of tumor physiology. Lower oxygen pressure (below 5-10 mm Hg) because of disorganized vasculature causes acute hypoxia in solid tumors.[3, 4] Hypoxic tumors are significantly resistant to the traditional chemotherapy and because of this hypoxic tumors are seen to have lower cure rate.[5, 6] On the other hand, hypoxia induces enhanced nitric oxide (NO) production at the tumor.[7-10] NO is the major signaling and effector molecule being produced in response to hypoxia to improve blood flow and oxygen supply (vasodilation).[11, 12] NO produced in tumor cell is known for tumor progression by induction of tumour-cell invasion, proliferation and the expression of angiogenic factors.[13-15] Therefore, the design of the probe which can image two factors specific for tumour environment (hypoxia and NO) is of great interest for biological applications, especially as only few dual-analyte probes have so far been successfully used in biology.[16-18] In addition, if the system is able to release active drug on the earmarked area (identified by image-guidance by hypoxia and NO detection) in a controlled manner (e.g. by light), it could function as both a dual-analyte probe and a prodrug.

For targeting hypoxia, nitroaromatics were frequently used as a bioreductive moiety since they undergo rapid reductive metabolism to produce aminoaromatics in hypoxic environment (**Scheme 1a**).[19-21] This efficient metabolic reduction can only occur in the tumor cells because severe hypoxia is rarely found in the healthy tissues.[22] On another note, the most common strategy to develop NO probes is based on the use of *o*-diamino aromatics (**Scheme 1b**).[23-25] These species react with an oxidation product of NO (N_2O_3) to furnish triazole moieties, an electron deficient moiety.[26, 27] This leads to a modulation of electronic distribution of the fluorophore thereby causing an alteration in the emission behavior. By the detection of both the unique biochemical alterations (hypoxia and NO) of tumor microenvironment, the exact location of tumor and clear discrimination between healthy and diseased cells can be achieved. However, still there is no literature available where both hypoxia and NO detection have been demonstrated by a single system.[18] Henceforth, we thought to design a single component prodrug system for the detection of hypoxia and NO by clubbing the aforementioned strategies (**Scheme 1c**). In addition, our designed system can be able to deliver anticancer agent upon irradiation of light.

Here, we have developed a simple coumarin based dual channel system, which is able to serve three purposes: (i)

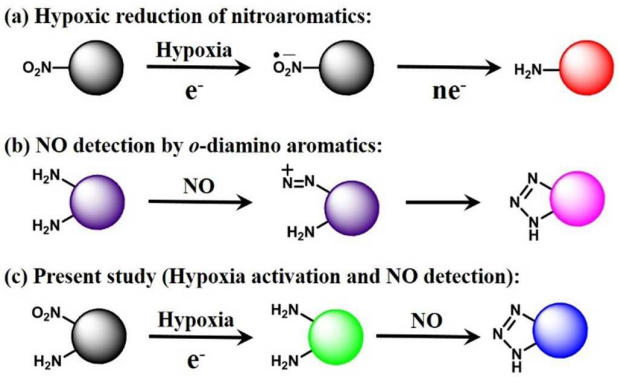

Scheme 1: Schematic representation of (a) Hypoxia detection strategy by nitroaromatics, (b) NO detection strategy of *o*-diamino aromatics and (c) present study (hypoxia and NO detection). Different colour represents different response of fluorophore.

[a] *Department of Chemistry, Indian Institute of technology Kharagpur, Kharagpur-721302, India. E-mail: ndpradeep@chem.iitkgp.ernet.in*
[b] *School of Medical Science and Technology, Indian Institute of Technology Kharagpur, Kharagpur-721302, India*

View Article Online
DOI: 10.1039/C8CC01854E

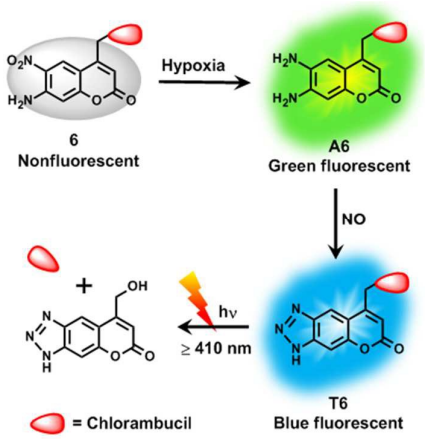

Scheme 2: Working protocol of conjugate **6**.

detection of hypoxic environment, (ii) act as a NO fluorescent probe and (iii) can deliver antitumor agent upon photoirradiation. When our system (**6**) enters into hypoxic environment, it undergoes reductive metabolism to produce the activated diaminocoumarin (**A6**). **A6** exhibits green fluorescence and acts as fluorescent probe for NO. Then, **A6** reacts with the NO present in the tumor cell and produces the new fluorescent phototrigger triazolocoumarin (**T6**), which exhibits blue fluorescence. Then, blue colour can be used as guiding mark of the hypoxia and NO positive areas, which could then be irradiated leading to a photorelease of the drug (**Scheme 2**).

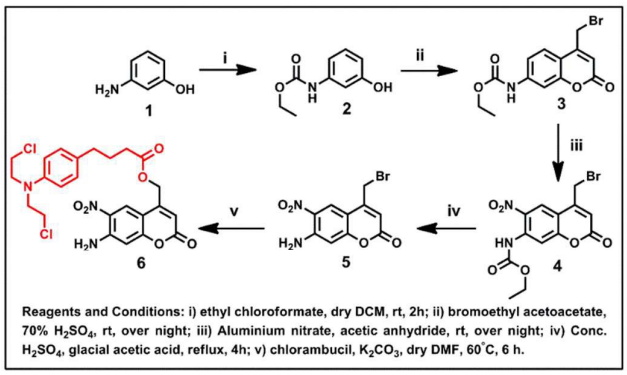

Scheme 3: Synthetic procedure of **6**.

Synthesis of the compound **6** was carried out according to the procedure depicted in **scheme 3**. Compound **3** was prepared by following the procedure described in our earlier work.[28] Nitration of **3** was carried out by treating **3** with aluminium nitrate and acetic anhydride at room temperature to produce **4**. The deprotection of **4** in presence of conc. H_2SO_4 and glacial acetic acid led to compound **5**. Finally, esterification of **5** with anticancer drug chlorambucil furnished coumarin-chlorambucil conjugate **6**. The products described in each step were characterized by NMR (^{1}H & ^{13}C) spectroscopy and mass spectrometry (**Figure S1 to S9**).

The UV spectrum shown in the **Figure S10** reveals that conjugate **6** has absorption maxima at 410 nm. Conjugate **6** exhibits very weak fluorescence intensity with a fluorescence

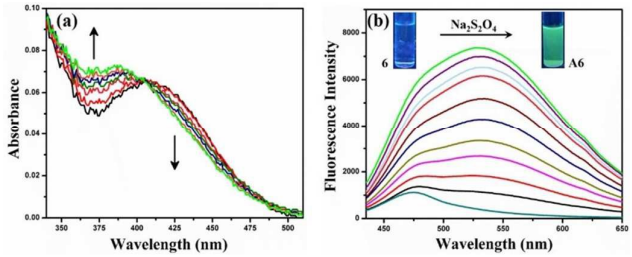

Figure 1: (a) Absorption spectral change and (b) fluorescence spectral change of **6** (1×10^{-5} M) in MeOH-PBS buffer (30:70) during addition of $Na_2S_2O_4$ (10 eqv).

quantum yield (Φ_f) = 0.01 (**Figure 1a**). The responses of **6** against hypoxia and NO was monitored by UV-Vis and fluorescence spectroscopy under physiological conditions (methanol : PBS buffer = 30 : 70, pH = 7.4). $Na_2S_2O_4$ was used as a reducing agent. During the addition of $Na_2S_2O_4$, the absorption maxima blue shifted from 410 nm to 387 nm (**Figure 1a**). An isosbestic point was noted at 407 nm. The inherent fluorescence of coumarin was rapidly recovered in the due course of addition of $Na_2S_2O_4$ (10 eqv), giving rise to a 55-fold fluorescence enhancement (Φ_f = 0.55, **Figure 1b**). After addition of $Na_2S_2O_4$, green fluorescence was observed with an emission maxima at around 535 nm. The same observation was noted in case of emission behaviour, when 6 was treated with bacterial nitroreductase enzyme (**Figure S11**). According to the well-established reaction mechanism,[29] the observed spectral change might be attributable to the formation of **A6**.

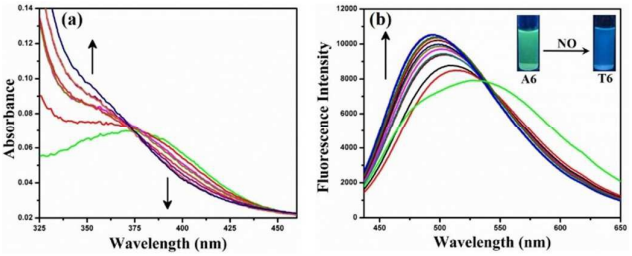

Figure 2: (a) Absorption spectral change and (b) fluorescence spectral change of **A6** (pretreated 6 with $Na_2S_2O_4$, 1×10^{-5} M) in MeOH-PBS buffer (30:70) during the addition of NO.

Next, introduction of an excess amount (500 eqv.) of NO donor (DEA-NANOate) resulted in a blue shift of the absorption maxima of **A6** from 387 nm to 355 nm with an isosbestic point at 372 nm (**Figure 2a**). The emission behaviour also showed a gradual blue shift of the 533 nm maxima with increase in the intensity (**Figure 2b**). This might be attributable to the formation of the blue triazolocoumarin (**T6**). The formation of **A6 and T6** were confirmed by RP-HPLC (reverse phase high performance liquid chromatography, **Figure S12**) and ESI-MS analysis (**Figure S13 to S15**).

The selective fluorescence activation of **6** by hypoxia over other biological reductants like dithiothreitol (DTT), glutathione (GSH), cysteine (Cys), homocysteine (Hcy), and β-Nicotinamide adenine dinucleotide (NADH) was also examined. Significant fluorescence modulation (**Figure S16**) was noted only upon addition of $Na_2S_2O_4$, indicating clear selectivity of **6** toward hypoxia in the cellular milieu. Further, we evaluated the specificity of **A6** for NO. We screened a wide variety of

View Article Online
DOI: 10.1039/C8CC01854E

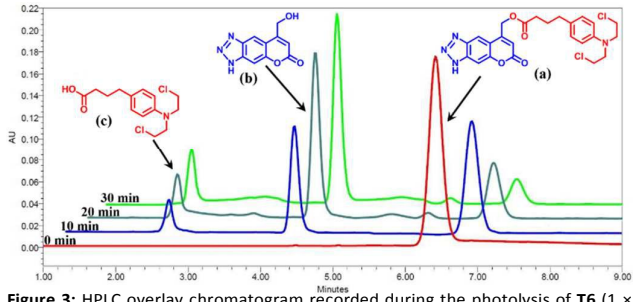

Figure 3: HPLC overlay chromatogram recorded during the photolysis of **T6** (1 × 10^{-4} M) using visible light (≥ 410 nm) ACN-water mixture. a = **T6**, b = **HO-T6** and c = released chlorambucil.

possible competitive species, reactive oxygen and nitrogen species (ROS or RNS) including H_2O_2, ClO^-, $O_2^{\cdot -}$, OH^-, $^1O_2$, NO_3^-, NO_2^-, ascorbic acid (AA), and dehydroascorbic acid (DHA). **A6** did not elicit any noticeable change in the emission spectrum except for NO suggesting high selectivity of **A6** for NO (**Figure S17**). The detection limit of NO by conjugate **A6** was found to be 24 nM (**Figure S18**).

The photorelease ability of in-situ generated **T6** was examined by exposing an ACN-water binary solution of **T6** (1×10^{-4} M) in visible light (≥ 410 nm) by medium pressure Hg-lamp using a suitable UV cut off filter (1 M $NaNO_2$ solution). The time course of the photolysis was monitored by RP-HPLC (**Figure 3**). Continual depletion of the peak at retention time (t_R) 6.42 min with increasing irradiation time denotes the photodecomposition of **T6**. On the other hand, appearance and gradual enhancement of two new peaks at t_R 4.43 min and 2.65 min indicate the photoproduct hydroxy-triazolocoumarin (**HO-T6**) and the released antitumor drug chlorambucil, which was further supported by ESI-MS (**Figure S19** & **S20**).

T6 showed a great control over the photoresponsive drug release when they were exposed to the periodic light and dark conditions, indicating light is entirely responsible for the release (**Figure S21a**). Upto 90% drug release was monitored, which occurred within 45 min of visible (≥ 410 nm) light irradiation (**Figure S21b**). Further, photochemical quantum yield of **T6** was calculated to be 0.04 (**Figure S22**).

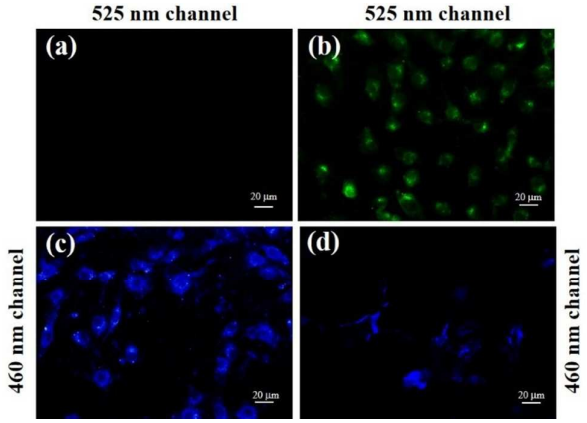

Figure 4: (a) Cellular fluorescence image of HeLa cells after incubated with **6**, (b) cells pretreated with **6** were kept in hypoxic condition, (c) hypoxic cells pretreated with 6 were incubated with NO and (d) after visible light (≥ 410 nm) irradiation. Excitation wavelength for imaging experiment was 400 nm. Each image was collected on different samples.

Now, we intended to investigate the hypoxia activated fluorescence activation, NO detection and photoregulated drug release ability of **6** *in vitro* using HeLa cell line. Conjugate **6** was internalized into the cancer cells and kept 6 h for hypoxic incubation. The green fluorescent cells in **Figure 4b** showed the clear activation of **6** under hypoxia condition. Next, the **6**-pretreated hypoxic HeLa cells were incubated with NO for another 6 h. After the treatment of NO, the cells exhibited blue coloured fluorescence indicating the formation of **T6** in the cellular milieu (**Figure 4c**). Then, the blue fluorescent cells were irradiated with visible light (≥ 410 nm) to release the anticancer drug chlorambucil. Increased round cell population after 30 min of photoirradiation indicates the cell death (**Figure 4d & S23**). The cellular fluorescence intensities at the above mentioned conditions were also quantified (**Figure S24**).

The anticancer efficacy of **6** was evaluated using MTT[30] (MTT= 3-(4,5-dimethylthiazol-2-yl)-2,5-diphenyltetrazolium bromide, a yellow tetrazole) assay against HeLa cell line. Percent of cell viability of **6, A6, T6, HO-T6** and chlorambucil have been depicted in **Figure S25a** (before photolysis). The cytotoxicity of **T6** is lower than chlorambucil at any given concentration. In contrast, after photolysis **T6** exhibited higher cytotoxicity than free chlorambucil indicating efficient release of chlorambucil inside the cell (**Figure S25b**). Additionally, **HO-T6** showed insignificant cell death both before and after photolysis, which clearly indicates that released chlorambucil is solely responsible for the cytotoxicity. Moreover, increased cytotoxicity was noted with increasing time of irradiation (**Figure S25c**), which confirms the controlled delivery of the anticancer agent. Further, highest level of cytotoxicity was observed after 45 min of photoirradiation.

While **T6** is the most probable light-activated pro-drug form in the case when hypoxia and NO are both present, in fact both **6** and **A6** can also act as phototriggers. Photolysis experiments in a cuvette showed that **6** and **A6** release 90% of the drug after 27 min and 73 min of irradiation with the visible light ((≥ 410 nm), respectively (**Figure S26**) which is comparable to the efficiency of drug release by **T6** (45 min). This is also in line with the photo-induced toxicity of **6** and **A6** in HeLa cells (**Figure S27**), which is in fact similar to the one observed for **T6**. This fact, however, does not interfere with the potential practical application of **6** as both dual-analyte probe and a photo-induced drug delivery system, as the irradiation could be applied selectively only to the areas stained in blue, and therefore positive for the presence of hypoxia and NO.

In summary, our newly developed coumarin-based single system system performed as a dual channel sensor (for hypoxia and NO) and delivered the antitumor drug chlorambucil in a photoregulated manner. Interestingly, good biocompatibility, ample sensitivity towards hypoxia and NO, great spatiotemporal precision over the drug delivery make our system an appreciable dual channel sensor and drug delivery vehicle. As such it also becomes one of the very few biocompatible dual-target probes and one of the first tools to

View Article Online
DOI: 10.1039/C8CC01854E

combine biochemical dual-gating with photocontrolled release of the drug, which is of high demand in biological studies.

Notes and references

We thank DST-SERB for the financial support. Sandipan Biswas is thankful to UGC-New Delhi and Y. Rajesh is thankful to DST for the fellowship.

1 W. R. Wilson and M. P. Hay, *Nature reviews. Cancer*, 2011, **11**, 393-410.
2 J. J. Yeh and W. Y. Kim, *J Clin Oncol*, 2015, **33**, 1505-1508.
3 S. M. Evans and C. J. Koch, *Cancer letters*, 2003, **195**, 1-16.
4 J. M. Brown and W. R. Wilson, *Nature reviews. Cancer*, 2004, **4**, 437-447.
5 P. Vaupel and A. Mayer, *Cancer metastasis reviews*, 2007, **26**, 225-239.
6 S. J. Lunt, N. Chaudary and R. P. Hill, *Clinical & experimental metastasis*, 2009, **26**, 19-34.
7 N. Burrows, G. Cane, M. Robson, E. Gaude, W. J. Howat, P. W. Szlosarek, R. B. Pedley, C. Frezza, M. Ashcroft and P. H. Maxwell, *Scientific reports*, 2016, **6**, 22950.
8 O. P. Mishra, S. Zanelli, S. T. Ohnishi and M. Delivoria-Papadopoulos, *Neurochemical Research*, 2000, **25**, 1559-1565.
9 R. Chowdhury, L. C. Godoy, A. Thiantanawat, L. J. Trudel, W. M. Deen and G. N. Wogan, *Chemical research in toxicology*, 2012, **25**, 2194-2202.
10 S. Pervin, R. Singh, E. Hernandez, G. Wu and G. Chaudhuri, *Cancer research*, 2007, **67**, 289-299.
11 M. Umbrello, A. Dyson, M. Feelisch and M. Singer, *Antioxidants & redox signaling*, 2013, **19**, 1690-1710.
12 A. Galkin, A. Higgs and S. Moncada, *Essays in biochemistry*, 2007, **43**, 29-42.
13 P. K. Lala and C. Chakraborty, *The Lancet. Oncology*, 2001, **2**, 149-156.
14 D. C. Jenkins, I. G. Charles, L. L. Thomsen, D. W. Moss, L. S. Holmes, S. A. Baylis, P. Rhodes, K. Westmore, P. C. Emson and S. Moncada, *Proceedings of the National Academy of Sciences of the United States of America*, 1995, **92**, 4392-4396.
15 L. L. Thomsen and D. W. Miles, *Cancer metastasis reviews*, 1998, **17**, 107-118.
16 M. Prost and J. Hasserodt, *Chemical Communications*, 2014, **50**, 14896-14899.
17 Y.-Q. Sun, J. Liu, H. Zhang, Y. Huo, X. Lv, Y. Shi and W. Guo, *J Am Chem Soc*, 2014, **136**, 12520-12523.
18 J. L. Kolanowski, F. Liu and E. J. New, *Chemical Society Reviews*, 2018, **47**, 195-208.
19 M. Tercel, G. J. Atwell, S. Yang, R. J. Stevenson, K. J. Botting, M. Boyd, E. Smith, R. F. Anderson, W. A. Denny, W. R. Wilson and F. B. Pruijn, *Journal of Medicinal Chemistry*, 2009, **52**, 7258-7272.
20 L. J. O'Connor, C. Cazares-Korner, J. Saha, C. N. Evans, M. R. Stratford, E. M. Hammond and S. J. Conway, *Nature protocols*, 2016, **11**, 781-794.
21 L. Cui, Y. Zhong, W. Zhu, Y. Xu, Q. Du, X. Wang, X. Qian and Y. Xiao, *Organic Letters*, 2011, **13**, 928-931.
22 Q. N. Lin, C. Y. Bao, Y. L. Yang, Q. N. Liang, D. S. Zhang, S. Y. Cheng and L. Y. Zhu, *Adv Mater*, 2013, **25**, 1981-1986.
23 H. Yu, Y. Xiao and L. Jin, *J Am Chem Soc*, 2012, **134**, 17486-17489.
24 C. Yu, Y. Wu, F. Zeng and S. Wu, *Journal of Materials Chemistry B*, 2013, **1**, 4152-4159.
25 N. G. Zhegalova, G. Gonzales and M. Y. Berezin, *Organic & Biomolecular Chemistry*, 2013, **11**, 8228-8234.
26 M. M. Tarpey, D. A. Wink and M. B. Grisham, *American journal of physiology. Regulatory, integrative and comparative physiology*, 2004, **286**, R431-444.
27 Y. Q. Sun, J. Liu, H. Zhang, Y. Huo, X. Lv, Y. Shi and W. Guo, *J Am Chem Soc*, 2014, **136**, 12520-12523.
28 S. Atta, A. Jana, R. Ananthakirshnan and P. S. Narayana Dhuleep, *Journal of Agricultural and Food Chemistry*, 2010, **58**, 11844-11851.
29 T. Thambi, V. G. Deepagan, H. Y. Yoon, H. S. Han, S. H. Kim, S. Son, D. G. Jo, C. H. Ahn, Y. D. Suh, K. Kim, I. C. Kwon, D. S. Lee and J. H. Park, *Biomaterials*, 2014, **35**, 1735-1743.
30 T. Mosmann, *Journal of immunological methods*, 1983, **65**, 55-63.

View Article Online
DOI: 10.1039/C8CC01854E

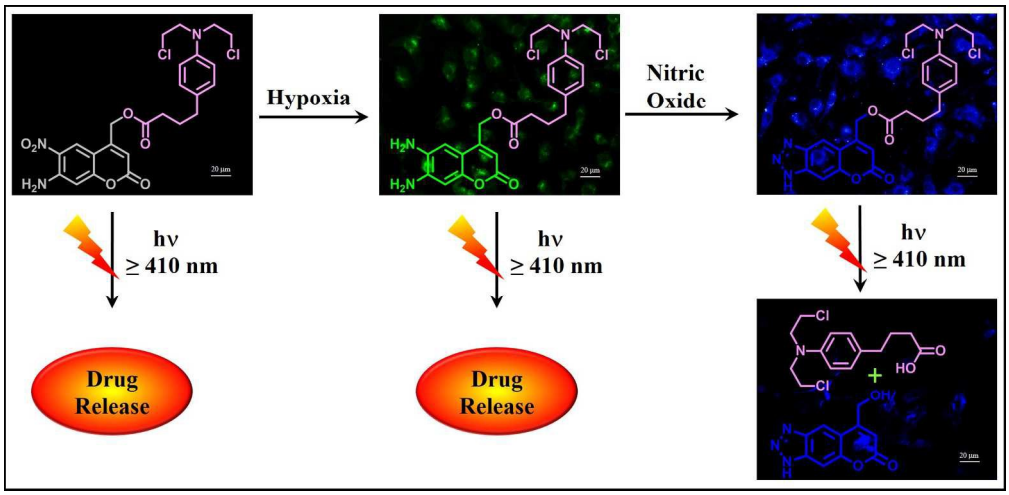

362x175mm (150 x 150 DPI)